314 *J. Phys. Chem. A* **2005,** *109,* 314−319

On the Titanium Oxide Neutral Cluster Distribution in the Gas Phase: Detection through 118 nm Single-Photon and 193 nm Multiphoton Ionization

Yoshiyuki Matsuda and Elliot R. Bernstein*

Department of Chemistry, Colorado State University, Fort Collins, Colorado 80523-1872

Received: October 20, 2004

Titanium oxide clusters are generated in a supersonic expansion by laser ablation of the metal and reaction with oxygen (0.1−6%) in He expansion gas. Mass spectra of the titanium oxide clusters are observed by photoionization with lasers of three different wavelengths: 118, 193, and 355 nm. Only the 118 nm (10.5 eV) light can ionize Ti_mO_n neutral clusters without fragmentation. Both the 193 nm (6.4 eV) and 355 nm (3.5 eV) multiphoton ionization cause fragmentation of the neutral clusters during the ionization process and, thus, can complicate the determination of the stable neutral Ti_mO_n gas-phase species. Employing 118 nm single-photon ionization and line-width data, the Ti_mO_{2m} and Ti_mO_{2m+1} series are found to be the most stable neutral cluster species for high oxygen content in the expansion gas. Fragmentation during the multiphoton ionization process for 193 nm light yields the cluster ions $Ti_mO^+_{2m-1,-2}$. These ions are formed by the loss of one or two oxygen atoms from $Ti_mO_{2m,2m+1}$ neutral species. The dominant cluster growth process is suggested to be through the addition of TiO_2 species. For low oxygen content (<2%) in the expansion gas, oxygen-deficient clusters of the form $Ti_mO_{2m-1,-2}$ are also observed. These latter series are not fragmented by the 193 nm ionization process.

I. Introduction

Interest in metal oxide clusters has been motivated by two fundamental issues: a desire to explain their geometric and electronic structures and the use of these species to aid in the elucidation of heterogeneous catalytic reactions and mechanisms.[1] Various spectroscopic studies[2−7] have been reported for small clusters, but large clusters can have many isomers, a very high density of electronic, vibrational, and rotational states, and are easily fragmented in the ionization detection process. Mass spectroscopy of metal oxide clusters can provide overall information on the stable neutral gas-phase species, the neutral cluster distribution, and the growth processes for cluster formation. For the elucidation of neutral cluster properties and distributions, one must ionize the gas-phase clusters in order to use mass spectroscopy as a detection technique. One of the major problems associated with the study of neutral clusters and their properties is that clusters may fragment during the electron- or photon-generated ionization process, and the identification of the neutral parent cluster can be difficult. In the past, covariance mapping of the mass spectral data has been applied to circumvent this loss of information.[5d,e]

Ionization thresholds for metal oxide clusters typically are found in the range 7−10 eV for small clusters; larger clusters can have lower ionization energies but are often in low abundance.[8−10] Specifically, the ionization energies of titanium oxide clusters are obtained both theoretically[9] and experimentally.[10] TiO, Ti_mO_{2m} ($m = 1, 2, 3$), and TiO_3 have calculated ionization energies between 6.5 and 9.7 eV, and experimentally, these ionization energies are found to be between 6.5 and 10.5 eV by electron impact and photoelectron studies. Laser radiation of 118 nm (10.5 eV/photon) is, therefore, sufficient for single-photon ionization of nearly all metal oxide clusters.[8−10] The 118 nm light is of sufficiently low intensity that multiphoton ionization/fragmentation processes are not probable. The TiO bond is given as ca. 160 kcal/mol (7 eV), and a TiO terminal bond should be between 5 and 7 eV in a cluster with oxygen-bridged titanium atoms. Thus, neither fragmentation nor insufficient single-photon energy should distort the mass spectral results obtained for the neutral cluster distribution through 118 nm ionization, assuming that the ionization cross-section is roughly constant over the distribution of small $m \leq 20$ clusters.

Light (118 nm) has been employed to ionize C_n,[11] methanol,[12] and ethanol[12] clusters and radicals,[13] and we have used 118 nm light to ionize, without fragmentation, iron oxide,[8a] copper oxide,[8b] and copper oxide hydride,[8b] zirconium oxide,[8c] and vanadium oxide[8d] clusters. In most instances, 118 nm ionization reveals different series of clusters than can be observed with 193 nm ionization, and on the basis of both experimental and theoretical results,[8] the 118 nm spectra reveal the neutral cluster distribution.

Mass spectra of titanium oxide clusters have been reported previously, employing 193 nm laser ionization[5d] and infrared resonant multiphoton ionization.[3a] In both spectra, no signal is observed for the series $(TiO_2)_n$. The 193 nm spectra show the dominant series of clusters to be $Ti_mO^+_{2m-1}$ and $Ti_mO^+_{2m-2}$. According to a covariance analysis of these mass spectral features,[5d] the observed cluster ions are related to one another by a growth process. The series $Ti_mO_{2m-1,-2}$ was thereby suggested to be the dominant clusters in the neutral cluster distribution.

In the present study of gas-phase neutral titanium oxide clusters, both 118 nm single-photon ionization and 193 and 355 nm multiphoton ionization techniques are employed to detect the clusters. Mass spectra are also measured as a function of oxygen content (0.1−6% O_2/He) in the expansion/reaction gas

---

* E-mail: erb@lamar.colostate.edu. Phone: 970-491-6347. Fax: 970-491-1801.

10.1021/jp040670h CCC: $30.25

used to generate the clusters. For an expansion gas mixture with more than 2% O_2 in He (saturated O_2 growth conditions) at ca. 100 psig, Ti_mO_{2m} and Ti_mO_{2m+1} are the two dominant cluster series observed employing 118 nm laser ionization. The averaged mass spectral feature fwhm for these clusters is ~10 ns (the seeded laser line width). This is strong evidence that cluster fragmentation does not occur under these conditions and that the stable neutral cluster series Ti_mO_{2m} and Ti_mO_{2m+1} are observed.

On the other hand, the $Ti_mO_{2m-1,-2}$ series are observed by 193 nm with complete absence of the $Ti_mO_{2m,2m+1}$ series, with 2−6% O_2 in the expansion/reaction gas. Comparison of mass spectra generated by 118 and 193 nm laser light shows that the fragmentation reaction for 193 nm ionization is

$$Ti_mO_{2m,2m+1} \xrightarrow[193\text{ nm}]{} Ti_mO_{2m-1,-2} + 1, 2, \text{ or } 3\text{ O}$$

and that this fragmentation is complete for all useful powers of 193 nm laser light, leaving no cluster ions of the two neutral series $Ti_mO_{2m,2m+1}$ detected.

II. Experimental Procedures

The apparatus and procedures for this work have been discussed in detail previously,[5d,8a] so only a brief description of the experiments will be given here. Titanium oxide clusters are made by 532 nm laser ablation of the metal into a stream of 0.1−6.0% O_2 in He. The reaction/expansion gas at 100 psig is introduced by a pulse valve (R. M. Jordan Co.) through a 0.8 mm orifice into a 2 mm diameter, 60 mm long channel. The titanium foil used in the ablation process is purchased from Aldrich Chemical Co.

The resulting titanium oxide clusters cool through expansion of the gas into a vacuum chamber and pass through a 2 mm aperture skimmer into the ionization region of a time-of-flight mass spectrometer (TOFMS). The neutral titanium oxide clusters are ionized by a laser for detection and mass analysis. Three different laser light sources are employed for the neutral Ti_mO_n cluster ionization: 355 nm (third harmonic of a seeded Nd:YAG laser), 193 nm (ArF excimer laser), and 118 nm (third harmonic of 355 nm Nd:YAG laser light). The ninth harmonic (118 nm) of the seeded Nd:YAG laser is generated in a 1:10 mixture of Xe/Ar from ca. 100−500 Torr pressure. Valve and laser timing and TOF mass spectral data collection are accomplished as described previously.[5d,8a]

III. Results and Disscussion

III-1. Neutral Cluster Distribution of Titanium Oxide Clusters. Figure 1 presents the TOF mass spectrum of Ti_mO_n clusters generated by different compositions of the reaction/expansion gas O_2/He and detected employing 118 nm ionization. The range of oxygen in the gas mixture is (a) 6%, (b) 4%, (c) 2%, (d) 0.5%, and (e) 0.1%. Mass peaks of Ti_mO_{2m} and Ti_mO_{2m+1} are observed by 118 nm ionization. Ti and TiO peaks are mainly due to ionization by residual 355 nm light at the ionization region. Spectra (a), (b), and (c) do not contain the other 355 nm ionized components. $Ti_mO_{2m-1,-2}$ peaks include both 355 and 118 nm ionization components. Structure around each identified cluster mass peak is due to the isotopic abundances of titanium metal. The most abundant isotope of titanium has a mass equal to that of three oxygen atoms, and thus, careful assignment of the features is necessary. The features can be identified through an analysis of the relative isotopic ratios for the various possible cluster masses. To see this, Figure 2 presents an expanded spectrum of Ti_2O_4 and Ti_3O_6 generated with 2% O_2/98% He reaction/expansion gas; one can clearly observe the titanium isotope structure for the neutral clusters employing 118 nm single-photon ionization. The structure of the cluster mass features is due to statistical combinations of isotopes of titanium. As shown in Figure 2, the intensity ratio between the central, most intense peak and the neighboring,

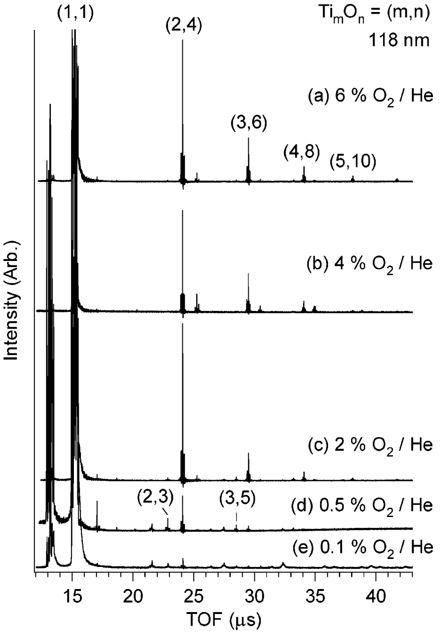

Figure 1. TOF mass spectra of titanium oxide clusters measured by 118 nm ionization. Each of the five spectra is generated with a different composition of O_2/He reaction/expansion gas mixture: (a) 6%, (b) 4%, (c) 2%, (d) 0.5%, and (e) 0.1% O_2. To generate 118 nm light, 355 nm light at 24 mJ/pulse and 200 Torr of Xe/Ar (1:10 mixture) are used. Conditions are maximized for detection of larger clusters.

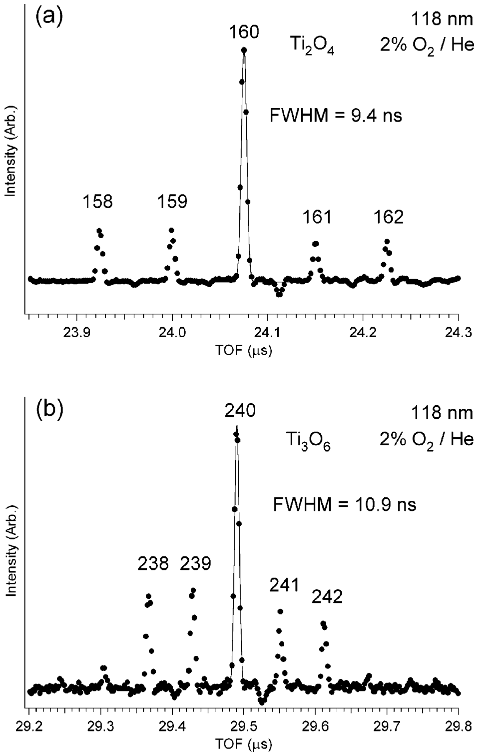

Figure 2. Expanded mass spectra for masses around the clusters (a) Ti_2O_4 and (b) Ti_3O_6. fwhm (full width at half-maximum) of mass peaks obtained by fitting Gaussian function to the indicated features are given in nanoseconds. Each mass peak is assigned by its mass number.

medium intense peaks is different for each of the clusters Ti_2O_4 and Ti_3O_6. Estimates of the expected cluster isotopic ratios are in agreement with the observed intensity ratios displayed in Figure 2. Thus, the mass peaks of the clusters can be assigned through their isotopic structure with no confusion from the accidental degeneracy between ^{48}Ti and three ^{16}O.

As shown in Figure 2, averaged (2000 laser pulses) line widths (fwhm) of the observed cluster ions with 118 nm light are ∼10 ns (the laser pulse width) based on a Gaussian curve fit to the experimental data. If a cluster fragments during or following the ionization process, while the species is still within the extraction/acceleration region of the TOFMS, the width of the associated detected mass feature can broaden and present a tail to longer times. The single ion features (ca. 8 mV as measured on an oscilloscope) have a width of ca. 2 ns for each laser pulse (approximately ion detector electron transit time) and an arrival time distribution as anticipated by the overall Gaussian shape of the averaged mass signal.[8c,d] Thus, the 10 ns averaged mass spectral feature width indicates that fragmentation does not occur in the time range ~ 1 ns $\leq t \leq \sim 1$ μs (from the time we can resolve to the time ions take to leave the ionization/extraction region of the TOFMS).

Therefore, as can be seen in Figure 1, for high oxygen content in the expansion gas (2%, 4%, 6% O_2/He), the most intense titanium oxide clusters have the stoichiometry Ti_mO_{2m} and Ti_mO_{2m+1}. On the other hand, as the oxygen content in the expansion gas drops below 1%, clusters of the forms Ti_mO_{2m-1} and Ti_mO_{2m-2} begin to appear in (and eventually dominate) the mass spectrum, and cluster growth kinetics dominate the neutral cluster distribution, and the Ti_mO_{2m} peak intensity decreases.

Rice−Ramsperger−Kassel−Marcus (RRKM) (and RRK) calculations of cluster vibrational predissociation times, experimental and theoretical ionization energies and binding energies,[9,10] mass spectral feature line width data, laser intensity calculations, and reasonable assumptions about ionzation cross-sections at 10.5 eV photon energy, all lead to the conclusion that the 118 nm ionization mass spectra of Ti_mO_n reflect the neutral cluster distribution for this system.

Oxygen-rich clusters such as TiO_3, TiO_4, Ti_2O_6, and so on are observed for high oxygen content in the expansion gas (≥2%), employing single-photon 118 nm nonfragmenting ionization. Thus, as calculated in ref 13, the ionization energies of these clusters are less than 10.5 eV. Additionally, the ionization cross-sections for the Ti_mO_n clusters appear to be similar.

With more than 2% O_2 present in the reaction/expansion gas, the $Ti_mO_{2m,2m+1}$ cluster series are the stable (not growth kinetics controlled) neutral cluster species. Clusters containing fewer oxygen atoms must be kinetically controlled in the growth process: they must cool before they can react completely with oxygen molecules.

III-2. Multiphoton Fragmentation and Ionization. A single photon of 193 nm (6.4 eV) radiation is not energetic enough to ionize most neutral metal oxide clusters. Thus, cluster ionization at this wavelength for mass spectroscopy detection of the neutral clusters must be, in general, through a mechanism that involves the absorption of at least two photons. During the multiphoton ionization process by a nanosecond light pulse, at least two processes can be responsible for cluster ionization: (1) a cluster can absorb a photon through low-lying electronic states and relax back to the ground electronic state many times, thus heating the cluster until thermionic emission occurs, and (2) vertical absorption of two or more photons can occur without rapid relaxation between absorption steps for both neutral and/or ionic species. In either case, fragmentation of the cluster is likely.

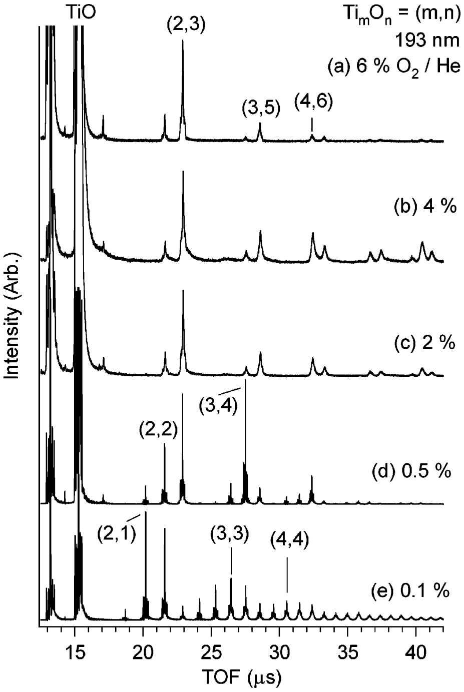

Figure 3. TOF mass spectra of titanium oxide clusters detected by 193 nm ionization with different compositions of O_2. These spectra correspond to those measured by 118 nm ionization shown in Figure 1.

Ti_mO_n clusters can also be ionized by 193 nm light, and Figure 3 presents the results of 193-nm-generated mass spectra of Ti_mO_n clusters for different concentrations of O_2 in the reaction/expansion gas. Figure 3 corresponds to Figure 1 for all experimental conditions except ionization laser wavelength. Figure 3c is essentially the same as that reported by ref 5d. In spectra 3a,b,c, the main mass features are from the series Ti_mO_{2m-1} and Ti_mO_{2m-2} ions. Ti_mO_{2m} and Ti_mO_{2m+1} are the mass features observed by 118 nm single-photon ionization for 2%, 4%, and 6% O_2 in the reaction/expansion gas. With lower oxygen concentration (0.1% and 0.5%), more oxygen-deficient clusters are observed in the 193 nm spectrum (Figure 3d,e).

With more than 2% O_2 in the reaction/expansion gas, the broadening of the mass spectral features becomes severe, and almost no Ti isotope structure can be observed. The mass spectral features for $Ti_mO^+_{2m-1,-2}$ ions are sharper for low O_2 concentration (fwhm ≈ 25 ns) in the expansion/reaction gas than for high O_2 concentration (fwhm ≈ 70 ns) in the expansion/reaction gas. The reason for this line width change with O_2 concentration is that, at high oxygen concentration in the expansion/reaction gas, $Ti_mO_{2m,2m+1}$ clusters are present and are fragmented by 193 nm multiphoton ionization into the $Ti_mO^+_{2m-1,-2}$ mass channels.

The TOF mass spectra obtained with different powers of 193 nm laser ionization for a 2% O_2/98% He reaction/expansion gas are presented in Figure 4a. Unlike other systems we have recently studied,[8c] these spectra do not change with laser power except to reduce uniformly in overall intensity as the power is reduced. This implies that neutral cluster fragmentation using 193 nm radiation for ionization cannot be avoided under our experimental conditions. Figure 4b shows the TOF mass spectra for Ti_mO_n clusters measured with 2% O_2/98% He and 193 nm ionization as a function of ionization laser timing relative to the nozzle opening and laser ablation time. By changing the

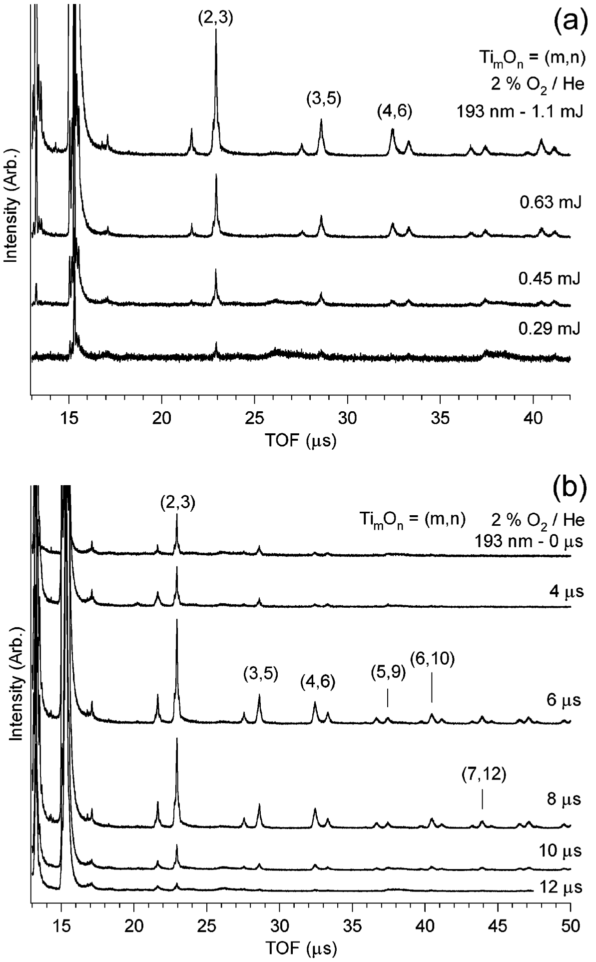

Figure 4. (a) TOF mass spectra of titanium oxide clusters detected by different energy/pulse 193 nm laser ionization and 2% O_2/He reaction/expansion gas. (b) TOF mass spectra of titanium oxide clusters observed with different 193 nm ionization laser timings and 2% O_2/He reaction/expansion gas. The number of microseconds indicated is the delay time for the ionization laser with respect to that employed to detect the spectrum initially (top). The same general trends are observed by 118 nm ionization.

ionization laser timing, the observed cluster distribution can be changed from more intense small clusters to more intense larger clusters; however, the relative cluster distribution patterns remain fixed with 193 nm ionization, because they are dominated by cluster fragmentation. With 118 nm ionization, the relative intensity of the Ti_mO_{2m} and Ti_2O_{2m+1} cluster series changes with ionization laser timing, as the two series must not be homogeneously distributed in the expansion beam.

The following question arises for the cluster fragmentation process with 193 nm ionization: Is the fragmentation "local", that is, $Ti_mO_{2m,2m+1} \rightarrow Ti_mO^+_{2m-1}$ and/or $Ti_mO^+_{2m-2}$ + 1, 2, or 3 O, or is it more general, with $Ti_mO_{2m,2m+1} \rightarrow Ti_{m-x}O_{2m-y} + Ti_xO_y$? From the study of iron oxide,[8a] copper oxide,[8b] and zirconium oxide clusters,[8c] we found that, on the basis of line width data, these clusters, upon multiphoton ionization, lose O atoms only, and not M_xO_y fragments. The same seems to be true for the case of the $Ti_mO_{2m,2m+1}$ cluster series. This conclusion follows from the fact that the only observed clusters with 193 nm multiphoton ionization are the oxygen-deficient ones, $Ti_mO_{2m-1,2m-2}$: if fragmentation generating TiO or TiO_2 occurs, then $Ti_mO^+_{2m,2m+1,2m+2}$ cluster ions should be observed. Additionally, as argued for Zr_mO_{2m} clusters,[5e,8c] the loss of an M_xO_y unit is not energetically or entropically favorable. Sequential loss of M_xO_y and nO ($n > 2$) should not be energetically possible for the laser intensities employed in these studies. This fragmentation trend is also consistent with the results of covariance mapping studies of Zr_mO_n clusters.[5e]

For less than 2% O_2 in the expansion/reaction gas, cluster growth is kinetically controlled, and the $Ti_mO_{2m,2m+1}$ series cannot form. Under such oxygen-deficient conditions for cluster growth, the mass spectral peak widths generated by 193 nm ionization are ca. 25 ns. The $Ti_mO_{2m-1,-2}$ series must be stable to fragmentation to lower-mass forms. These widths are much smaller than those found for similar features at high oxygen concentration for cluster growth, but not as small as those found for similar features detected by single-photon 118 nm ionization (~10 ns, compare to Figure 2). This residual line width difference at the two laser wavelengths for ionization can have three contributions: (1) the ArF laser (193 nm) pulse time profile could be larger than that of the Nd:YAG (118 nm) laser, (2) the 193 nm laser light is not as tightly focused as the 118 nm light, ~2 mm × 0.1 mm versus ca. 50 μm, and (3) perhaps some residual cluster fragmentation is still present. This latter point can be, in particular, a contributing factor to the line widths for $Ti_2O_2^+$ and Ti_2O_3, as Ti_2O_4 neutral is present in the beam even at these lower oxygen percentages in the expansion/reaction gas. In fact, the line widths for $Ti_2O_2^+$ and $Ti_2O_3^+$ detected with 193 nm ionization are 24 and 35 ns, respectively, while those for other nearby clusters (Ti_2O, Ti_2O_4, Ti_3O_2) are ca. 21.5 ns.

III-3. Cluster Growth Processes. Upon the basis of ionization laser/ablation laser timing, and variation of the various experimental parameters (e.g., O_2%, ion steering plate voltages, etc.), the most intense nonfragmented cluster observed through 118 nm single-photon ionization is TiO_2. High-energy/pulse (~25 mJ/pulse) 355 nm ionization generates Ti and TiO features while fragmenting TiO_2 and larger (Ti_mO_n, $m > 1$, $n > 2$) stable species. At such high pulse energies for low-energy photons, many photons (perhaps more than 10)[14] are probably absorbed, and cluster fragmentation can include loss of TiO and other Ti_xO_y species. The presence of Ti and TiO in the mass spectrum must then be mostly through fragmentation of larger clusters. Given the abundance of the TiO_2 neutral, the cluster growth process is through the TiO_2 building block ($TiO_2 + TiO_2 + ... \rightarrow (TiO_2)_n$) with the possible addition of an O or a TiO_3 to generate the Ti_mO_{2m+1} series.

Berstein and co-workers[5d] report a covariance mapping study of $Ti_mO_n^+$ clusters and suggest a growth mechanism for them. Spectra of ref 5d are based on 193 nm ionization, and thus, the Ti_mO_{2m-1} and Ti_mO_{2m-2} cluster series (at ca. 2% O_2 in the reaction/expansion gas) are identified, which are fragments of the neutral cluster series Ti_mO_{2m} and Ti_mO_{2m+1}. In the covariance mapping data analysis and modeling of ref 5d,e, positive values of covariance correspond to a cluster growth ($Ti_xO_y + TiO_2 \rightarrow Ti_{x+1}O_{y+2}$, ...) correlation, and negative values of covariance correspond to a cluster fragmentation (parent−daughter) correlation. The analysis[5d] correctly shows a positive covariance between mass features in Ti_mO_n cluster ion mass spectra detected by 193 nm multiphoton fragmenting ionization. These authors conclude that the cluster pattern they observe is a growth pattern (positive covariance at low laser power) and that the Ti_mO_{2m-1} and Ti_mO_{2m-2} series are growth-generated and represent the neutral cluster distribution. They are correct to suggest these fragmented clusters are related to one another by a growth mechanism, but we now know they do not represent the stable neutral cluster distribution (i.e., Ti_mO_{2m}, Ti_mO_{2m+1}). These oxygen-deficient fragmented clusters are growth-related because their parents (Ti_mO_{2m} and Ti_mO_{2m+1}) are. Fragmentation correlations are lost in the 193-nm-ionization-detected spectrum because of total fragmentation; that is, one can presume that clusters of the series (Ti_mO_{2m}, Ti_mO_{2m+1}) and (Ti_mO_{2m-1}, Ti_mO_{2m-2}) would have negative covariances if they could be simultaneously observed at the same O_2 concentration in the reaction/expansion gas mixture. This also supports the conclusion that fragmentation is local for 193 nm ionization, because the loss of M_xO_y units from parent clusters would yield fragmentation correlations between observed daughter species.

Covariance mapping is certainly a useful technique for the analysis of mass spectral cluster features and for generating a relation between observed features. Covariance mapping yields useful information concerning neutral cluster growth and fragmentation in the ionization process. Single-photon (118 nm) ionization is perhaps the best way to avoid fragmentation and thus determine the neutral cluster distribution. The neutral cluster distribution is the cluster population in the preionized beam and, thus, the one that is essential to know for any preionization reactivity and/or catalytic behavior one can study with gas-phase clusters. Single-photon near-threshold ionization is the most certain way to get this information.

III-4. Comparison of Titanium Oxide and Zirconium Oxide Clusters. Titanium and zirconium belong to the same group (4) of the periodic table and thus can be expected, in general, to have similar gas-phase cluster or molecular properties. Here, we list and discuss both similarities and differences between these two sets of clusters:

First, the two most stable neutral cluster species for both elements are of the forms M_mO_{2m} and M_mO_{2m+1} (M = Ti, Zr). Nonetheless, we find additional neutral clusters for zirconium oxide of the forms Zr_mO_{2m+2}, Zr_mO_{2m+3}, and Zr_mO_{2m+4}. The only comparable oxygen-rich clusters observed for titanium oxides are TiO_3, TiO_4, and Ti_2O_6, but these features are of very low intensity.

Second, for both systems, 193 and 355 nm ionization cause fragmentation of the clusters by loss of oxygen, generating the following reactions:

$$Ti_mO_{2m,2m+1} \rightarrow Ti_mO^+_{2m-1,-2} + 1, 2, \text{ or } 3\ O$$

$$Zr_mO_{2m,2m+1} \rightarrow Zr_mO^+_{2m-1} + 1 \text{ or } 2\ O$$

Zirconium oxide clusters do not generate $Zr_mO^+_{2m-2}$ species upon fragmenting ionization.

Third, mass spectra of zirconium oxide clusters, ionized by 193 nm light at ca. 1 mJ/pulse, consist only of cluster ions of the form $Zr_mO^+_{2m-1}$, while at low energy/pulse (0.15−0.6 mJ/pulse), $Zr_mO^+_{2m,2m-1}$ ($m \geq 5$) are detected. In the case of titanium oxide clusters, $Ti_mO_{2m-1,2m-2}$ and no $Ti_mO^+_{2m,2m+1}$ clusters are observed by 193 nm ionization with 0.3−1.2 mJ/pulse.

Fourth, under oxygen-deficient conditions, only Ti_mO_{2m-1} and Ti_mO_{2m-2} neutral clusters are generated, and these are stable to 193 nm ionization at ca. 1 mJ/pulse. Thus, the oxygen-deficient titanium oxide clusters are quite stable toward fragmentation upon ionization.

Finally, the covariance mapping data of ref 5d,e are consistent with the third and fourth points. The covariance matrix elements for titanium oxide clusters are always positive independent of laser energy/pulse, while those for zirconium oxide clusters evidence both positive and negative contributions as the laser energy/pulse is lowered.

V. Conclusions

We employ two methods of ionization to detect titanium oxide gas-phase clusters created by laser ablation of the metal into a mixture of 0.1−6% O_2 in He: single-photon low-intensity 118 nm (10.5 eV) ionization, and multiphoton high-intensity 193 nm (6.4 eV) and 355 nm (3.5 eV) ionization.

Observed mass spectral averaged features obtained by 118 nm laser ionization have a TOF fwhm of ca. 10 ns; individual ion signals can have fwhms as small as ca. 1.7 ns. These line widths are expected for single-photon nonfragmenting ionization under our experimental conditions. The neutral cluster Ti_mO_n distribution is revealed from this TOF mass spectrum; the two neutral cluster series Ti_mO_{2m} and Ti_mO_{2m+1} are found to be the stable ones under conditions of saturated growth O_2 content in the beam (≥2% O_2). The main cluster growth mechanism in the ablation/expansion process is suggested to be $TiO_2 + TiO_2 + ... = (TiO_2)_m$ for the series Ti_mO_{2m} with an additional O atom acquired through the addition of either O or TiO_3 to the growing T_mO_{2m} clusters to generate the Ti_mO_{2m+1} neutral cluster series.

By employing 193 nm multiphoton ionization for the Ti_mO_n clusters, the stable neutral oxygen-rich clusters of the forms Ti_mO_{2m} and Ti_mO_{2m+1} suffer dissociation and lose oxygen as follows:

$$Ti_mO_{2m}, Ti_mO_{2m+1} \rightarrow Ti_mO^+_{2m-1}, Ti_mO^+_{2m-2} + (1, 2, \text{ or } 3)\ O$$

On the other hand, oxygen-poor clusters Ti_mO_{2m-1} and Ti_mO_{2m-2} (generated mostly from reaction/expansion gas mixtures with less than 2% O_2) are mostly ionized without fragmentation by 193 nm ionization. These cluster features have fwhms of ca. 25 ns and are about 2.5 times as broad as the features observed with 118 nm single-photon ionization, but not as broad as features (ca. 70 ns) that derive from fragmentation of the parent species $Ti_mO_{2m,2m+1}$. This residual line width for nonfragmented cluster features in 193 nm versus the 118-nm-ionization-detected mass spectra can be due to a broader time pulse width for the ArF laser than the Nd:YAG laser and a larger focal spot for the ArF laser beam than for the Nd:YAG-derived 118 nm beam.

The neutral cluster distribution can be determined in this way for both unsaturated and saturated O_2 growth conditions, yielding both kinetically controlled and stable metal oxide clusters, respectively. We are now in the process of using these neutral cluster beams to interact with small gas-phase molecules such as NO_x, CO, SO_2, H_2O, NH_3, and others to study the reactivity of neutral metal oxide clusters and their potential catalytic behavior.

Acknowledgment. These studies are supported in part by the US DOE, Basic Energy Sciences program.

References and Notes

(1) (a) Smalley, R. E. *CAMS Symposium on Molecular and Cluster Beam Science*; 1987; Chapter 7, p 76. (b) Hackett, P. A.; Mitchell, S. A.; Rayner, D. M.; Simard, B. In *Metal−Ligand Interactions*; Russo, R., Salahub, D. R., Eds.; Kluwer: Amsterdam, 1996; p 289. (c) Castleman, A. W., Jr.; Bowen, K. H., Jr. *J. Phys. Chem.* **1996**, *100*, 12911.

(2) (a) Suenram, R. D.; Lovas, F. J.; Fraser, G. T.; Matsumura, K. *J. Chem. Phys.* **1990**, *92*, 4724. (b) Brugh, D. J.; Suenram, R. D.; Stevens, W. J. *J. Chem. Phys.* **1999**, *111*, 3526. (c) Knight, L. B., Jr.; Babb, R.; Ray, M.; Banisaukas, T. J., III; Russon, L.; Dailey, R. S.; Davidson, E. R. *J. Chem. Phys.* **1996**, *105*, 10237.

(3) (a) von Helden, G.; van Heijnsbergen, D.; Meijer, G. *J. Phys. Chem. A* **2003**, *107*, 1671. (b) van Heijnsbergen, D.; von Helden, G.; Meijer, G.; Duncan, M. A. *J. Chem. Phys.* **2002**, *116*, 2400. (c) von Helden, G.; Kirilyuk, A.; van Heijnsbergen, D.; Sartakov, B.; Duncan, M. A.; Meijer, G. *Chem. Phys.* **2000**, 262, 31. (d) Chertihin G. V.; Andrews, L. *J. Phys. Chem.* **1995**, *99*, 6356.

(4) (a) Michalopoulos, D. L.; Geusic, M. E.; Langridge-Smith, P. R. R.; Smalley, R. E. *J. Chem. Phys.* **1984**, *80*, 3556. (b) Negishi, Y.; Nagao, S.; Nakamura, Y.; Kamei, S.; Nakajima, A.; Kaya, K. *Trans. Mater. Res. Soc. Jpn.* **2000**, *25*, 999. (c) Terasaki, A.; Breire, T. M.; Kulawik, M.; Minemoto, S.; Tono, K.; Matsushita, A.; Kondow, T. *J. Chem. Phys.* **2003**, *118*, 2180.

(5) (a) Riley, S. J. *Metal−Ligand Interactions: from Atoms, to Clusters, to Surfaces*; Kluwer Academic Publishers: The Netherlands, 1992; p 17. (b) Sakurai, M.; Watanabe, K.; Sumiyama, K.; Suzuki, K. *J. Chem. Phys.* **1999**, *111*, 235. (c) Cox, D. M.; Trevor, D. J.; Whetten, R. L.; Rohlfing, E. A.; Kaldor, A. *Phys. Rev. B* **1985**, *32*, 7290. (d) Foltin, M.; Stueber, G. J.; Bernstein, E. R. *J. Chem. Phys.* **1999**, *111*, 9577. (e) Foltin, M.; Stueber, G. J.; Bernstein, E. R. *J. Chem. Phys.* **2001**, *114*, 8971. (f) Shin, D. N.; Matsuda, Y.; Bernstein, E. R. *J. Chem. Phys.* **2004**, *120*, 4150.

(6) (a) Wu, H.; Wang, L.-S. *J. Chem. Phys.* **1998**, *108*, 5310. Wu, H.; Wang, L.-S. *J. Chem. Phys.* **1997**, *107*, 8221. (b) Wu, H.; Desai, S. R.; Wang, L.-S. *J. Am. Chem. Soc.* **1996**, *118*, 5296. (c) Zhai, H.-J.; Wang, L.-S. *J. Chem. Phys.* **2002**, *117*, 7882. (d) Andrews, D. H.; Gianola, A. J.; Lineberger, W. C. *J. Chem. Phys.* **2002**, *117*, 4074. (e) Pramann, A.; Koyasu, K.; Nakajima, A.; Kaya, K. *J. Phys. Chem. A* **2002**, *106*, 4891.

(7) (a) Harrington, J.; Weisshaar, J. C. *J. Chem. Phys.* **1992**, *97*, 2809. (b) Aguire, F.; Husband, J.; Thompson, C. J.; Stringer, K. L.; Metz, R. B. *J. Chem. Phys.* **2003**, *119*, 10194.

(8) (a) Shin, D. N.; Matsuda, Y.; Bernstein, E. R. *J. Chem. Phys.* **2004**, *120*, 4157. (b) Matsuda, Y.; Shin, D. N.; Bernstein, E. R. *J. Chem. Phys.* **2004**, *120*, 4165. (c) Matsuda, Y.; Shin, D. N.; Bernstein, E. R. *J. Chem. Phys.* **2004**, *120*, 4142. (d) Matsuda, Y.; Bernstein. E. R. *J. Phys. Chem.*, to be submitted.

(9) Albaret, T.; Finocchi, F.; Noguera, C. *J. Chem. Phys.* **2000**, *113*, 2238.

(10) NIST Chemistry WebBook, NIST Standard Reference Database Number 69-March, 2003 Release: http://webbook.nist.gov/chemistry.

(11) (a) Kaizu, K.; Kohno, M.; Suzuki, S.; Shiromaru, H.; Moriwaki, T.; Achiba, Y. *J. Chem. Phys.* **1997**, *106*, 9954. (b) Wakabayashi, T.; Momose, T.; Shida, T. *J. Chem. Phys.* **1999**, *111*, 6260.

(12) Shi, Y. J.; Consta, S.; Das, A. K.; Mallik, B.; Lacey, D.; Lipson, R. H. *J. Chem. Phys.* **2002**, *116*, 6990.

(13) (a) Fanourgakis, G. S.; Shi, Y. J.; Consta, S.; Lipson, R. H. *J. Chem. Phys.* **2003**, *119*, 6597. (b) Shi, Y. J.; Consta, S.; Das, A. K.; Mallik, B.; Lacey, D.; Lipson, R. H. *J. Chem. Phys.* **2002**, *116*, 6990. (c) Chambreau, S. D.; Zhang, J.; Traeger, J. C.; Morton, T. H. *Int. J. Mass Spectrosc.* **2000**, *199*, 17. (d) Yen, M.-W.; Johnson, P. M.; White, M. G. *J. Chem. Phys.* **1993**, *99*, 126.

(14) Nieman, G. C.; Parks, E. K.; Richtsmeier, S. C.; Liu, K.; Pobo, L. G.; Riley, S. J. *High Temp. Sci.* **1986**, *22*, 115.